Hindawi Publishing Corporation
EURASIP Journal on Wireless Communications and Networking
Volume 2008, Article ID 458785, 8 pages
doi:10.1155/2008/458785

Research Article

Joint Multilevel Turbo Equalization and Continuous Phase Frequency Shift Keying

Oguz Bayat,[1] Niyazi Odabasioglu,[2] Onur Osman,[3] Osman N. Ucan,[2] Masoud Salehi,[4] and Bahram Shafai[4]

[1] *Electronics and Communication Engineering Department, Beykent University, Buyukcekmece, 34500 Istanbul, Turkey*
[2] *Electrical and Electronics Engineering Department, Istanbul University, Avcilar, 34320 Istanbul, Turkey*
[3] *Electronics and Telecommunications Engineering Department, Engineering Faculty, Halic University, Sisli, 34381 Istanbul, Turkey*
[4] *Electrical and Computer Engineering, Northeastern University, 360 Huntington Avenue, Boston, MA 02115, USA*

Correspondence should be addressed to Oguz Bayat, obayat@beykent.edu.tr

Received 2 May 2008; Revised 21 July 2008; Accepted 31 December 2008

Recommended by Huaiyu Dai

A novel type of turbo coded modulation scheme, called multilevel turbo coded-continuous phase frequency shift keying (MLTC-CPFSK), is designed to improve the overall bit error rate (BER) and bandwidth efficiency. Then, this scheme is combined with a new double decision feedback equalizer (DDFE) to remove the interference and to enhance BER performance for the intersymbol interference (ISI) channels. The entire communication scheme is called multilevel turbo equalization-continuous phase frequency shift keying (MLTEQ-CPFSK). In these schemes, parallel input data sequences are encoded using the multilevel scheme and mapped to CPFSK signals to obtain a powerful code with phase continuity over the air. The performances of both MLTC-CPFSK and MLTEQ-CPFSK systems were simulated over nonfrequency and frequency-selective channels, respectively. The superiority of the two level turbo codes with 4CPFSK modulation is shown against the trellis-coded 4CPFSK, multilevel convolutional coded 4CPFSK, and TTCM schemes. Finally, the bit error rate curve of MLTEQ-CPFSK system over Proakis B channel is depicted and ISI cancellation performance of DDFE equalizer is shown against linear and decision feedback equalizers

1. INTRODUCTION

With the development of the wireless communication industry, wireless data communications have become a very important research area for many scientists. As a result, tremendous improvements have occurred in coding, modulation, and signal processing subsystems to provide burst rates along with power efficiency at low bit error rates. First, conventional turbo code was found to be very attractive in the last decade [1], since turbo code reached theoretical limits in an iterative fashion at low signal-to-noise ratio with a cost of a low code rate and bandwidth expansion. Several years later, the compensation for bandwidth expansion and the low code rate was realized by applying multilevel and trellis-coded modulation to turbo code, known as multilevel turbo codes (MLTCs) [2, 3] and turbo trellis-coded modulation (TTCM) [4, 5], respectively, in the literature. These techniques increase the spectral efficiency of the coding via concatenating higher-order modulation using PSK or QAM modulations [6]; however, these communication models have phase jumps in their modulated signals. Continuous phase modulation (CPM) has explicit advantages in deep space and satellite communications, such as having low spectral occupancy property. Thus, to improve the bandwith usage further, MLTC design is concatenated and investigated with CPM modulation in this research.

MLTC is modeled by applying separate turbo encoders at each level. Each turbo encoder processes the information sequence simultaneously. For each level of the mutilevel encoder, there exists a corresponding decoder defined as a stage. The output of one stage is utilized at the decoder of the following stage in the decoding flow, known as multistage decoding [7].

The CPM model that is used with the MLTC is composed of a continuous-phase encoder (CPE) and a memoryless mapper (MM). The CPE is a convolutional encoder producing codeword sequences that are mapped onto waveforms by the MM, creating a continuous-phase signal. CPE-related schemes have better BER performance than systems using the traditional approach for a given number of trellis states

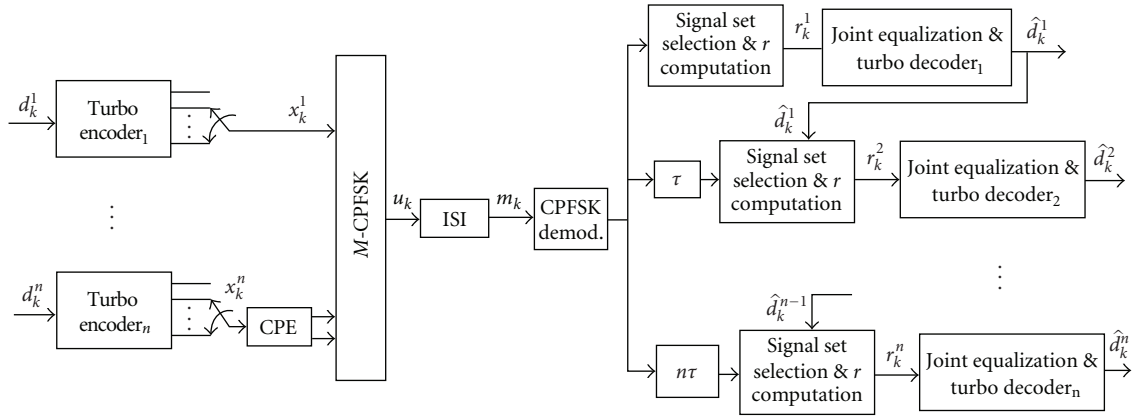

Figure 1: MLTEQ-CPFSK structure block diagram.

due to larger Euclidean distances. When the decomposed structure of CPM is considered, joint trellis coded and CPM, and joint multilevel convolutional code and CPM systems can be designed as in [8, 9].

For achieving a low bit error rate (BER) over a severe ISI channel, the double decision feedback equalization is designed for MLTC-CPFSK system [10–12]. It is well know that maximum a posteriori probability (MAP) and soft output Viterbi algorithm-based equalizers are very effective, but having very high complexity, which is not applicable to our design since our transmission scheme has high complexity. Performances of traditional low-complexity equalizers such as linear equalizer (LE) and decision feedback equalizers (DFE) are not effective under severe channel conditions. To close the performance gap between high- and low-complexity equalizers, DDFE is proposed and implemented into the MLTC-CPFSK system. Thus, the effect of a severe ISI channel is mitigated by the equalization process and then the equalized information passes through the MAP algorithm-based decoders which decode the two encoded streams by exchanging the soft decisions.

In this paper, Section 2 explains the design of multilevel turbo encoder with CPFSK modulation. Section 3 describes the DDFE-based turbo equalization receiver scheme. In Section 4,the performances of the proposed MLTC-CPFSK and MLTEQ-CPFSK schemes are presented over AWGN, Rician, Rayleigh, and Proakis B channels, respectively, and the conclusion is stated at the last section.

2. THE DESIGN OF MULTILEVEL TURBO ENCODER USING CPFSK

M-ary continuous phase frequency shift keying (M-CPFSK) is a special form of M dimensional CPM. In the literature, Rimoldi firstly derived the tilted-phase representation of CPM in [13], with the information-bearing phase given by

$$\phi(t,X) = 4\pi h \sum_{i=0}^{\infty} X_i q(t - iT). \tag{1}$$

The modulation index h is equal to J/P, where J and P are relatively prime integers. X is an input sequence of M-ary symbols, $X_i \in \{0, 1, 2, \ldots, M-1\}$ $i \geq 0$. T is the channel symbol period. In CPFSK design, modulation index $h = 1/2$ is considered and the frequency pulse is a rectangular pulse of duration LT and height $1/(2LT)$, yielding a linearly increasing/decreasing instantaneous phase $\phi(t, X)$. In this design, full response CPFSK modulator is considered. The phase response function $q(t)$ is a continuous and monotonically increasing function subject to the constraints

$$q(t) = \begin{cases} 0, & t \leq 0, \\ \dfrac{1}{2}, & t \geq LT, \end{cases} \tag{2}$$

where L is an integer that denotes the number of memory units in CPE. The phase response is usually defined in terms of the integral of a frequency pulse $g(t)$ of duration LT, that is, $q(t) = \int_{-\infty}^{t} g(\tau)d\tau$. For full response signaling L equals to 1, and for partial response systems L is greater than 1. Finally, the transmitted signal $u(t)$ is derived as

$$u(t,X) = \sqrt{\frac{2E_s}{T}} \cos\left(2\pi f_1 t + \phi(t,X) + \phi_0\right), \tag{3}$$

where f_1 is the asymmetric carrier frequency as $f_1 = f_c - h(M-1)/2T$ and f_c is the carrier frequency. E_s is the energy per channel symbol and ϕ_0 is the initial carrier phase. We assume that $f_1 T$ is an integer; this condition leads to a simplification when using the equivalent representation of the CPM waveform.

Multilevel turbo code using CPFSK modulation consists of many parallel turbo encoder/decoder levels. In Figure 1, high-level block diagram of designed transceiver is shown for n level case. There exists a binary turbo encoder at every level of the multilevel turbo encoder, and there is a continuous-phase encoder serially connected to the turbo encoder at the last level. Based on Rimoldi's model and the assumption in [13], CPE would be a convolutional encoder. In this model, the outside encoder is designed to maximize the Euclidean distance between output signals whereas CPE is used to shape the modulated signal's spectrum. In the CPFSK design, the state of CPE is binary and it changes with time. The phase of

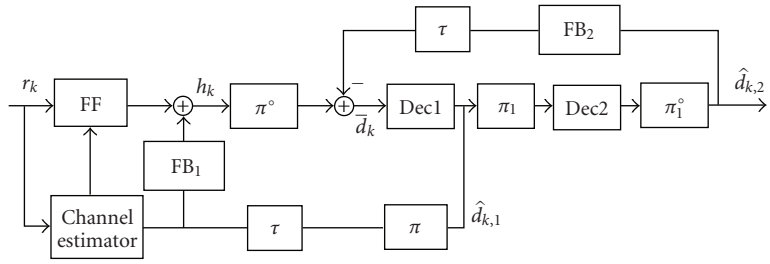

Figure 2: Joint DDFE and turbo decoder structure.

the modulated signal depends on the memoryless modulator. The first process of the transmitter is that the information sequence is converted from serial to parallel in the multilevel scheme. Then, each turbo encoder processes the information sequence simultaneously. Additionally, the outputs of the last turbo encoders are run through the CPE. The outputs of all encoders' outputs and CPE output are mapped to CPFSK signals. In Figure 4, the two-level multilevel turbo transmission system (2LTC-4CPFSK) is illustrated in detail since this research simulations were performed on a two-level model. In each level, a 1/3 turbo encoder is demonstrated with recursive systematic convolutional (RSC) encoders having memory size $M_s = 2$ as in Figure 4(a). For mapping the encoders' outputs to 4CPFSK signals, the first and second bits are taken from the first and second level of turbo encoder output, respectively. The third bit is obtained from the output of the CPE. Thus, based on the output of the encoders x_k^1, $x_{k,1}^2$, and $x_{k,2}^2$, the CPFSK modulated signals $u = \{u_0, u_1, u_2, u_3, u_4, u_5, u_6, u_7\}$ are transmitted at four different frequencies $f_1, f_1 + 1/2T$, $f_1 + 1/T$, and $f_1 + 3/2T$. The initial and ending physical tilted phases are 0 and π as shown in Figure 5. At the receiver, 4CPFSK signal constellation partitioning is optimized to provide low BER for AWGN and fading channels as in [9]. The signal set partitioning technique for 2LTC-4CPFSK signals is as follows: depending on the estimated output bit of the first-level turbo decoder is whether $x_k^1 = 0$ or $x_k^1 = 1$, $u_0^1 = \{u_0, u_1, u_4, u_5\}$ or $u_1^1 = \{u_2, u_3, u_6, u_7\}$ signal set is chosen, respectively. Then, depending on the estimated second-level turbo encoder output bit $\{x_{k,1}^2\}$ and the CPE output bit $\{x_{k,2}^2\}$, the transmitted signal is determined as shown in Figure 5.

3. TURBO EQUALIZATION RECEIVER SCHEME

For the kth symbol interval, a set of basis functions was used to find the coordinates in signal space and to form the vector u_k in each signaling interval. Let the transmitted MLTC-CPFSK symbol sequence be $\overline{u} = \{u_0, u_1, \ldots\}$ and the corresponding received sequence be $\overline{m} = \{m_0, m_1, \ldots\}$, where the kth received vector element equals to m_k. In this case, the channel output during the kth symbol interval can be expressed as

$$m_k = a_k u_k + n_k, \tag{4}$$

where n_k is kth noise vector element of the noise sequence $\overline{n} = \{n_0, n_1, \ldots\}$ and its elements are additive white Gaussian noise with an $N_0/2E_s$ power spectral density, Es is the signal energy per symbol, a_k is Rician fading amplitude, which varies by Rician probability distribution function as in

$$P(a) = 2a(1+K)e^{(-a^2(1+K)-K)} I_0\left[2\sqrt{K(1+K)}\right], \tag{5}$$

where K is the Rician factor in terms of dB. We assume that the demodulator operates over one symbol interval, which yields a discrete memoryless channel. At the receiver, the corrupted MLTC-CPFSK signals are processed by the demodulator and MAP decoder to extract the information sequence.

MLTEQ-CPFSK scheme is applied to Proakis B channel. This channel is time-invariant ISI channel having L_2 casual, L_1 anticasual terms and is known as severe ISI channel with 3 main taps and no precursor and postcursor taps [14]. The output of the channel is equal to

$$m_k = \sum_{i=-L_1}^{L_2} F_i u_{k-i} + n_k, \tag{6}$$

where F_k are the coefficients of the equivalent discrete channel.

After the M-CPFSK modulated signals are run through the channel, they are demodulated and then noisy demodulator outputs are evaluated for every equalization and decoding process. The following is the high-level summary of the equalization and decoding process. In the first step, the probabilities of received signal being zero and one is computed as in (7) and then, the probabilities are mapped to $\{-1, 1\}$ range via (8). In the second step, the computation of the equivalent discrete channel taps is explained when the channel conditions are known for the traditional decision feedback equalizer. In our application and real applications, the channel information is not known. Thus, the estimation process of the channel via LMS algorithm is performed and described. The coefficient vectors of the filters are defined from (14) and their adaptation is explained from (15). The DDFE equalization output is derived with (17). Finally, the equalized information is processed by the MAP decoder as in (18).

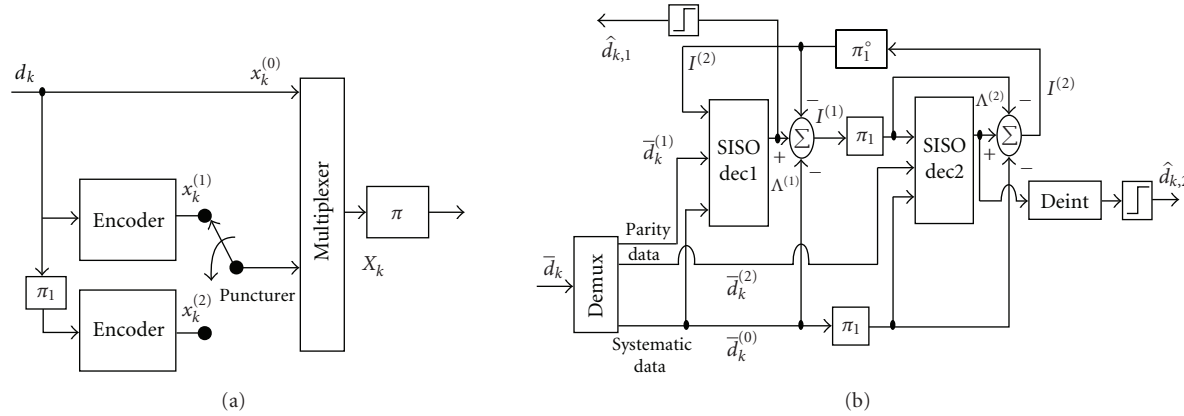

Figure 3: Turbo code structure: (a) turbo encoder structure, (b) turbo decoder structure.

At the receiver, the probabilities of the corrupted received signals being zero and one are computed as follows:

$$P_{k,0}^{st} = \sum_{j=0}^{(2M/2^{st})-1} P\left(m_k \mid u_{0,j}^{st}\right) \propto \sum_{j=0}^{(2M/2^{st})-1} e^{|m_k - u_{0,j}^{st}|^2/N_0},$$
$$P_{k,1}^{st} = \sum_{j=0}^{(2M/2^{st})-1} P\left(m_k \mid u_{1,j}^{st}\right) \propto \sum_{j=0}^{(2M/2^{st})-1} e^{|m_k - u_{1,j}^{st}|^2/N_0}, \tag{7}$$

where $P_{k,0}^{st}$ and $P_{k,1}^{st}$ indicate zero and one probabilities of the received signal at time k and stage st. The partitioning stage is equal to $st \in \{1, 2, \ldots, \log_2 M\}$. u_0^{st}, u_1^{st} are the selected signal sets at stage st.

In multilevel coding scheme, each digit of binary correspondence of CPFSK signals matches to one stage from the most significant to the least significant while the stage number increases. Signal set is partitioned into the subsets due to each binary digit matching stage depending on whether it is 0 or 1. After computing the one and zero probabilities, received signals are mapped to $\{-1, 1\}$ range and then sent to the equalization and decoding process at each level,

$$r_k^{st} = 1 - \frac{2 \cdot P_{k,0}^{st}}{P_{k,0}^{st} + P_{k,1}^{st}}. \tag{8}$$

As shown in Figure 2, DDFE structure mainly consists of 3 linear transversal filters: the feed forward (FF) filter, and two feedback filters (FB), a channel interleaver (π), deinterleaver (π°), and two delay components. The decoder structure is made of two interleavers (π_1), two deinterleavers (π_1°), a demultiplexer, and two soft input soft output (SISO) decoders which exchange priori information as indicated in more detail in Figure 3.

In order to reduce the notation of the equations and figures, the notation is not changed when the information is processed by the interleavers. Only the channel output feeds the equalizer at the first iteration, therefore, the equalizer uses training sequence to operate for the initial process. For further iterations, the FF filter is fed by the channel output and the channel estimator output. The channel estimator uses both the hard decision of the first decoder and the channel output to estimate the channel information. The first FB filter uses the hard decision of the first decoder ($\hat{d}_{k,1}$) whereas the second FB filter uses the hard decision of the second decoder ($\hat{d}_{k,2}$).

In order to perform the conventional DFE equalization, error propagation has to be ignored, which means $\hat{d} = d$. The coefficient of the equalizer is computed in [7] by using mean square error (MSE), which is based on the minimization of the difference between the equalized data ($\overline{d}_k$) and the hard decision of the first decoder ($\hat{d}_{k,1}$) as follows:

$$E\left|e_k\right|^2, \quad \text{where } e_k = \hat{d}_{k,1} - \overline{d}_k, \tag{9}$$

$$\overline{d}_k = \sum_{j=-L_1}^{0} v_j r_{k-j} - \sum_{j=1}^{L_2} w_j \hat{d}_{k,1-j}, \tag{10}$$

where L_1 and L_2 are the numbers of feedforward and feedback coefficients, respectively. v is the coefficient of the FF filter, where w is the coefficient of the FB filter. By using first orthogonality principle, the feedforward coefficients of the filter are computed. This principle yields to the following set of linear equations:

$$\sum_{j=-L_1}^{0} v_j \Gamma_{tj} = F_{-t}^*, \quad -L_1 \le t \le 0, \tag{11}$$

where

$$\Gamma_{tj} = \sum_{n=0}^{-t} F_n^* F_{n+t-j} + N_o \delta_{tj} \tag{12}$$

where $t, j = -L_1, \ldots, -1, 0$ and F is the channel tap. The coefficient of the FB filter is computed by the second orthogonality principle,

$$w_k = \sum_{j=-L_1}^{0} v_j F_{k-j}, \quad k = 1, 2, \ldots, L_2. \tag{13}$$

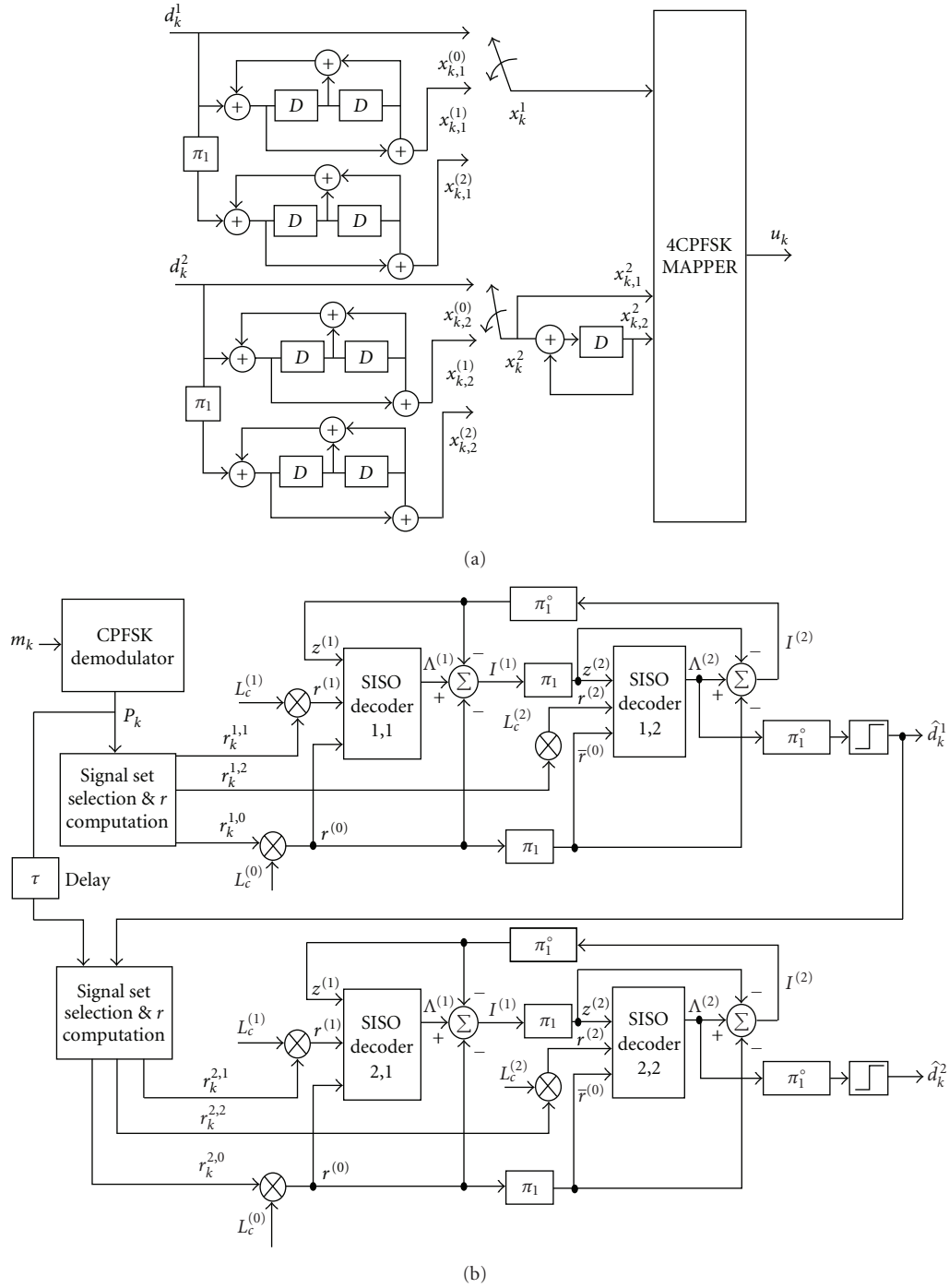

Figure 4: 2LTC-4CPFSK system for $M_s = 2$ and without equalization: (a) encoder structure, (b) decoder structure.

Since the equivalent discrete channel taps are unknown in most of the communication applications, the filter coefficient cannot be computed from the equation above.

We selected LMS algorithm to determine the filter coefficients because of its less complexity and high accuracy on time-invariant channels at large frame sizes. By LMS algorithm, the coefficients of channel and feedback filters are estimated from the corrupted transmitted signal and the hard decisions of the decoders after certain latency (τ) is introduced to the system. After the first iteration, the coefficient vectors of the FF, first FB, and second FBfilters are computed, respectively, as

$$\begin{aligned} V_k &= \left[v_{-L_1}(k), v_{-L_1+1}(k), \ldots, v_0(k)\right]^T, \\ W_k &= \left[w_1(k), w_2(k), \ldots, w_{L_2}(k)\right]^T, \\ Q_k &= \left[q_{L_2+1}(k), q_{L_2+2}(k), \ldots, q_{L_3+L_2+1}(k)\right]^T. \end{aligned} \tag{14}$$

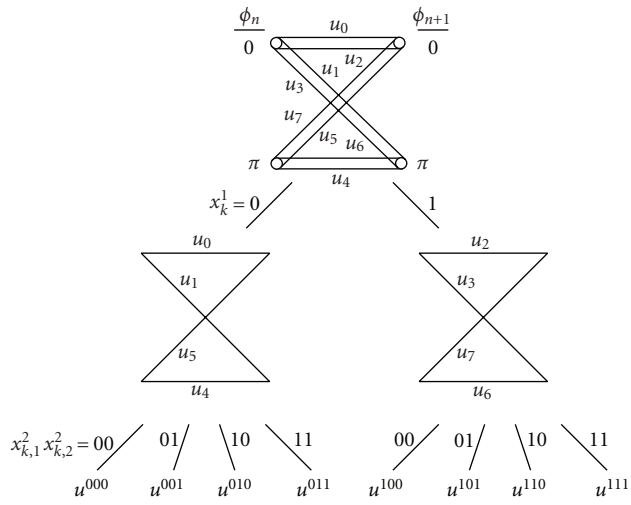

Figure 5: Set partitioning of 4CPFSK.

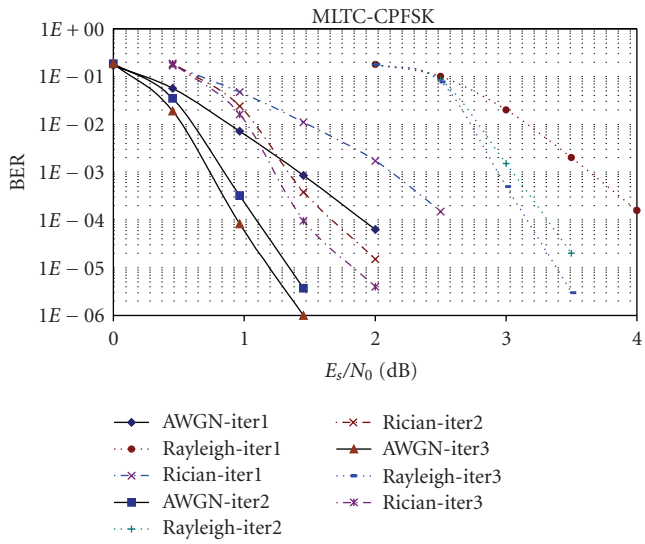

Figure 6: Performance of the two-level turbo coding system using 4CPFSK modulation, $N = 1024$.

In LMS algorithm, the coefficients of the FF and FB filters are adapted as follows:

$$\begin{aligned} V_{k+1} &= V_k + \Delta_V R_k(\hat{d}_{k,1} - r_k), \\ W_{k+1} &= W_k + \Delta_W \hat{D}_{k,1}(\hat{d}_{k,1} - h_k), \\ Q_{k+1} &= Q_k + \Delta_Q \hat{D}_{k,2}(\hat{d}_{k,2} - \overline{d}_k), \end{aligned} \tag{15}$$

where Δ is the step size of the LMS algorithm, and $R_k = [r_{k+L_1}(k), r_{k+L_1-1}(k), \ldots, r_k(k)]^T$ is the vector of the transmitted signal, and the vectors below are the hard-decision vectors of the decoders from the previous iteration,

$$\begin{aligned} \hat{D}_{k,1} &= [\hat{d}_{(k,1)+L_2}(k), \hat{d}_{(k,1)+L_2-1}(k), \ldots, \hat{d}_{(k,1)+1}(k)]^T, \\ \hat{D}_{k,2} &= [\hat{d}_{(k,2)+L_3+L_2+1}(k), \ldots, \hat{d}_{(k,2)+L_2+1}(k)]^T. \end{aligned} \tag{16}$$

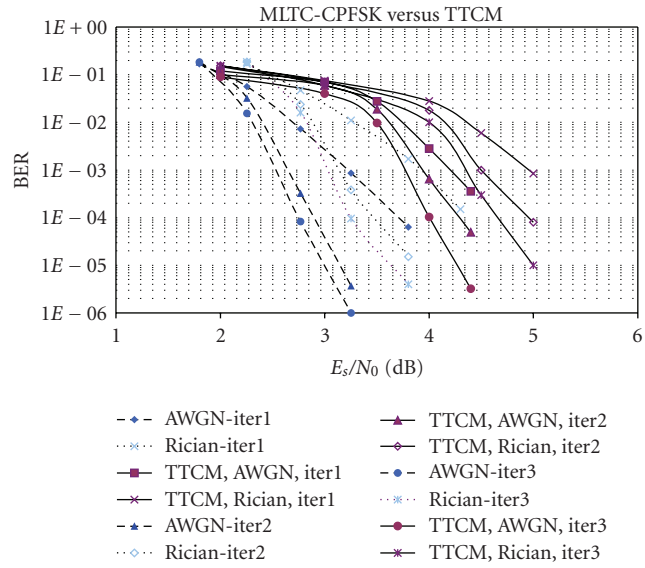

Figure 7: Performance comparison of 2LTC-4CPFSK and TTCM systems, $N = 1024$.

After the corrupted transmitted signals are filtered by FF and first FB filters as shown in (10), it is deinterleaved (h_k)and subtracted from the output of the second FB filter to obtain DDFE output ($\overline{d}_k$) as below,

$$\overline{d}_k = h_k - \sum_{L_2+1}^{L_3+L_2+1} q_k \hat{d}_{k,2}. \tag{17}$$

During the initializing period, the coefficients of the FF filter at the first iteration are estimated from the training sequence by the LMS criterion due to the fact that the hard decision of the decoder does not exist at the first iteration. Therefore, the DDFE structure behaves as a linear equalizer fed by the training sequence at the first iteration.

Eventually, the equalized information sequences ($\overline{d}_k$) are passed through the SISO decoders.In SISO decoders, the MAP algorithm calculates the a posteriori probability of each bit at each decoding process [15]. At the last iteration, hard decision is computed by using the second decoder output $\Lambda^{(2)}$ as follows:

$$\hat{d}_k = \begin{cases} 1, & \text{if } \Lambda^{(2)} \geq 0, \\ 0, & \text{if } \Lambda^{(2)} < 0. \end{cases} \tag{18}$$

4. SIMULATION RESULTS

The performance of the two-level turbo coded 4CPFSK system is shown by plotting the bit error rate versus signal-to-noise ratio in Figure 6. Joint two-level turbo code and 4CPFSK scheme with random interleaver size $N = 1024$, generator sequence (37, 21) in octal form, and overall rate 2/3 was simulated for AWGN, Rician (Rician fading parameter $K = 10$ dB) and Rayleigh channels. Then, the proposed 2LTC-4CPFSK scheme was compared to the known existing multilevel schemes using CPFSK showed in [8, 9], called ref-1 and ref-2, respectively. The code on reference one (ref-1) is

Table 1: Coding gains (in dB) over reference systems for $P_e = 10^{-4}$.

Iteration	Coding gains for 2LTC-4CPFSK over ref-1		
	AWGN channel	Rician channel (K = 10 dB)	Rayleigh channel
1	3.5	3.8	7.5
2	4.2	4.55	8.4
3	4.4	4.8	8.55
Coding gains for 2LTC-4CPFSK over system (S-5) in ref-2			
1	1	0.8	0.2
2	1.7	1.55	1.1
3	1.9	1.8	1.25

binary trellis-coded 4-ary CPFSK scheme with overall rate 2/3, and the code labeled (S-5) in reference two (ref-2) is the combined multilevel convolutional code and 4CPFSK. The proposed system has much better performance than ref-1 and satisfactory coding gain over ref-2 for all channel conditions as stated in Table 1. The comparison among these systems was revealed for the fixed bit error rate 10^{-4}. For instance, the coding gain under AWGN channel between MLTC-CPFSK and ref-1 is 3.3, 4.05, and 4.3 dB for iteration one to three, respectively.

The proposed 2LTC-CPFSK method was also compared with the bandwidth efficient TTCM scheme, which is shown in Figure 7. The TTCM model in [4] was simulated with 8 states, N = 1024, 2048 bits for overall rate 1 to provide the BER performance for AWGN and Rician (K = 10 dB) channels. To have a better comparison with TTCM model at the same overall rate, we have performed MLTC-CPFSK simulation with the same parameters as given above, except puncturing that used this time to achieve overall rate 1. The comparison indicates that MLTC-CPFSK system has 0.9, 1.2, and 1.3 dB coding gain against TTCM system for first, second, and third iterations, respectively, over AWGN channel. Also, our design has 1.7–2 dB gain over Rician channel. This important performance difference is achieved by MLTC-CPFSK system due to the fact that the concatenation of the powerful multilevel turbo codes and the CPE encoder yields higher Hamming distance and leads to good error performance for both AWGN and Rician channels.

The BER performance of 2LTEQ-4CPFSK is depicted over Proakis B channel for interleaver size N = 2048 frame size in Figure 8. Aggressive performance of the designed MLTEQ-CPFSK model was generated under severe ISI channel such as BER 10^{-5} was achieved at SNR 10.5 dB at the sixth iteration. It is illustrated that significant amount of gain is achieved at each iteration by reducing the frequency dispersive effects of Proakis B channel. DDFE equalizer has 0.8 dB and 2.1 dB gains at BER 10^{-5} over conventional DFE and minimum mean square sequence error-based LE equalizers, respectively. DDFE equalizer provides gain at a cost of introducing additional feedback filter and delay into the system when compared to the complexity of the DFE equalizer. The overall delay of the proposed systems will be minimized to be employed in some real applications; however, the proposed systems are suitable for mobile data communications, video, and audio broadcasting.

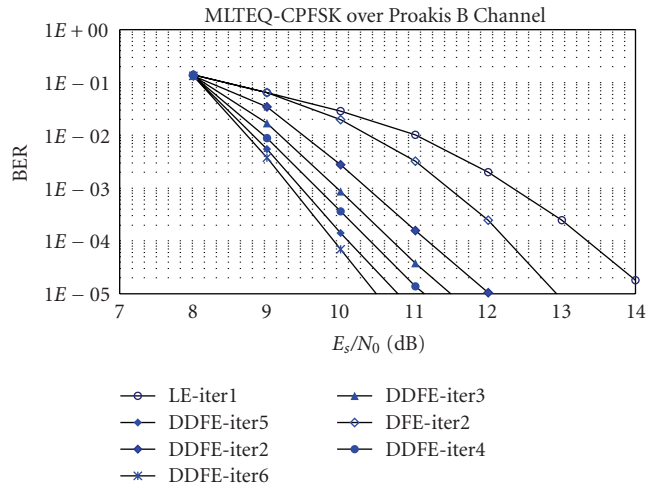

Figure 8: Performance of the two-level turbo equalization using 4CPFSK modulation over Proakis B channel, N = 2048.

5. CONCLUSION

We have presented multilevel turbo codes scheme with CPFSK modulation, and joint multilevel turbo equalization scheme with CPFSK modulation in this paper. MLTC-CPFSK design compensates the requirement of large frame size and high iteration number to obtain low BER at low SNR for turbo codes by adding complexity and slight latency due to the multistage structure. As shown in Figure 7, MLTC-CPFSK model achieves 10^{-5} BER performance at the third iteration when SNR equals to 3 dB and 3.7 dB for AWGN and Rician channels, respectively. When we compared our model with the well-known multilevel coded CPFSK and TTCM schemes in the literature, we observed important coding gains with the simulation results. Furthermore, low-complexity DDFE equalizer was designed and its good interference cancellation performance was presented against LE and DFE equalizers. Eventually, satisfactory performance results for MLTEQ-CPFSK scheme is demonstrated for severe ISI channels.

REFERENCES

[1] C. Berrou, A. Glavieux, and P. Thitimajshima, "Near Shannon limit error-correcting coding and decoding: turbo-codes (1)," in *Proceedings of IEEE International Conference on Communications (ICC '93)*, pp. 1064–1070, Geneva, Switzerland, May 1993.

[2] L. Papke and K. Fazel, "Combined multilevel turbo-code with MR-modulation," in *Proceedings of IEEE International Conference on Communication (ICC '95)*, vol. 2, pp. 668–672, Seattle, Wash, USA, June 1995.

[3] D. Divsalar and F. Pollara, "Multiple turbo codes," in *Proceedings of IEEE Military Communications Conference (MILCOM '95)*, vol. 1, pp. 279–285, San Diego, Calif, USA, November 1995.

[4] P. Robertson and T. Wörz, "Bandwidth-efficient turbo trellis-coded modulation using punctured component codes," *IEEE Journal on Selected Areas in Communications*, vol. 16, no. 2, pp. 206–218, 1998.

[5] W. J. Blackert and S. G. Wilson, "Turbo trellis coded modulation," in *Proceedings of the Conference on Information Signals and System (CISS '96)*, Princeton, NJ, USA, March 1996.

[6] U. Wachsmann, R. F. H. Fischer, and J. B. Huber, "Multilevel codes: theoretical concepts and practical design rules," *IEEE Transactions on Information Theory*, vol. 45, no. 5, pp. 1361–1391, 1999.

[7] O. Bayat, B. Shafai, and O. N. Ucan, "Iterative equalization of frequency selective channels," in *Proceedings of IEEE/Sarnoff Symposium on Advances in Wired and Wireless Communication*, pp. 33–36, Princeton, NJ, USA, April 2005.

[8] M. Naraghi-Pour, "Trellis codes for 4-ary continuous phase frequency shift keying," *IEEE Transactions on Communications*, vol. 41, no. 11, pp. 1582–1587, 1993.

[9] I. Altunbas and U. Aygolu, "Multilevel coded CPFSK systems for AWGN and fading channels," *IEEE Transactions on Communications*, vol. 48, no. 5, pp. 764–773, 2000.

[10] O. Bayat, B. Shafai, and O. N. Ucan, "Reduced state equalization of multilevel turbo coded signals," in *Proceedings of IEEE International Conference on Acoustics, Speech and Signal Processing (ICASSP '05)*, vol. 3, pp. 705–708, Philadelphia, Pa, USA, March 2005.

[11] O. Osman, O. N. Ucan, and N. Odabasioglu, "Performance of multilevel turbo codes with group partitioning over satellite channels," *IEE Proceedings: Communications*, vol. 152, no. 6, pp. 1055–1059, 2005.

[12] N. Odabasioglu and O. N. Ucan, "Multilevel turbo coded-continuous phase frequency shift keying (MLTC–CPFSK)," *Computers & Electrical Engineering*. In press.

[13] B. E. Rimoldi, "A decomposition approach to CPM," *IEEE Transactions on Information Theory*, vol. 34, no. 2, pp. 260–270, 1988.

[14] J. G. Proakis, *Digital Communications*, McGraw-Hill, New York, NY, USA, 4th edition, 2000.

[15] O. Bayat, A. Hisham, O. N. Ucan, and O. Osman, "Performance of turbo coded signals over fading channels," *Journal of Electrical & Electronics Engineering*, vol. 2, no. 1, pp. 417–422, 2002.